Charge accumulation and barrier formation at grain boundaries in ZnO decorated with bismuth



2002 J. Phys.: Condens. Matter 14 12717

(http://iopscience.iop.org/0953-8984/14/48/308)

INSTITUTE OF PHYSICS PUBLISHING JOURNAL OF PHYSICS: CONDENSED MATTER

J. Phys.: Condens. Matter **14** (2002) 12717–12724 PII: S0953-8984(02)54135-7

# Charge accumulation and barrier formation at grain boundaries in ZnO decorated with bismuth

**H S Domingos[1], J M Carlsson[2], P D Bristowe[1] and B Hellsing[2]**

[1] Department of Materials Science and Metallurgy, University of Cambridge, Pembroke Street, Cambridge CB2 3QZ, UK
[2] Experimental Physics, Chalmers and Göteborg University, SE-412 96, Gothenburg, Sweden

E-mail: pdb1000@cus.cam.ac.uk (P D Bristowe)

Received 1 October 2002
Published 22 November 2002
Online at stacks.iop.org/JPhysCM/14/12717

**Abstract**

Density functional plane-wave pseudopotential calculations have been performed on two high-angle grain boundaries in ZnO which have been decorated with various quantities of Bi. The results show that both grain boundaries, which have significantly different structures, can accommodate up to about 30% of substitutional Bi in qualitative agreement with experimental observations. The segregation of Bi to the boundaries results in local charge accumulation which is localized within Bi–Bi bonds or on Bi atoms. The charge accumulation in both boundaries results in fluctuations in potential across the interface and the formation of a barrier to electron transport. However, there is no evidence for a deep acceptor level usually associated with the Schottky barrier model. The present results suggest an alternative mechanism in which electrons are trapped in Bi–Bi bonds and depleted in an external field. However, defect states have not been ruled out and it is suggested that if they exist they are caused by more complex defects than those considered here.

(Some figures in this article are in colour only in the electronic version)

## 1. Introduction

Zinc oxide is a remarkably versatile material with applications in the pharmaceutical, food, paint, rubber and ceramic industries. Most recently it has been recognized as a potentially useful optoelectronic material because of its wide band gap, large exciton binding energy and the ease with which it can be grown into large single-crystal wafers [1]. However, its most common device application is probably the varistor which is typically used for overvoltage protection in electronic circuits and power distribution networks [2]. In this application the material is in polycrystalline form and prepared by liquid-phase sintering of ZnO powder with $Bi_2O_3$ and other additives. The resulting microstructure is complex but generally consists of large ZnO grains with polymorphs of $Bi_2O_3$ at the triple junctions and an adsorbed layer of

  

bismuth along the grain boundaries [3]. Sometimes a Bi-rich amorphous intergranular phase is also observed [4]. The polymorphs of $Bi_2O_3$ (typically $\alpha$-$Bi_2O_3$ or $\delta$-$Bi_2O_3$ depending on processing conditions) are not thought to influence the electrical properties of the material but act as sources of Bi which diffuses into the boundaries.

The diffusion of Bi into the grain boundaries is a key factor determining the functionality of the varistor. The doped grain boundaries create an electrostatic barrier to charge transport and trap electrons. The release of the electrons at the breakdown voltage produces the material's non-linear $I$–$V$ characteristic which is essential for varistor function. To explain this behaviour a double-Schottky-barrier model has been proposed, whose microscopic origin is interface states of acceptor type in the band gap [5]. Although this model is widely accepted, the chemical nature of the acceptor states remains unresolved. Experimental and theoretical studies suggest that the grain boundaries themselves are not electrically active [6, 7]. Recent calculations have also suggested that grain boundaries containing native point defects do not form deep trap states either [8]. To investigate the possibility that Bi segregation creates the necessary potential barriers and electron traps, we have performed a series of *ab initio* density functional calculations on two model grain boundary systems. The two boundaries studied have significantly different structures and orientations and are decorated with up to one monolayer of Bi. The results show that although Bi segregation produces charge accumulation at the boundaries and the formation of potential barriers, there is no evidence for a deep defect level of acceptor type as proposed in the Schottky barrier model.

## 2. Computational method

The calculations are based on density functional theory [9] using the PW-91 generalized gradient (GGA) exchange–correlation functional [10]. The wavefunctions are expanded in a plane-wave basis set and the use of ultrasoft pseudopotentials [11] allows a plane-wave energy cut-off of 340 eV. The Brillouin zone is sampled at $k$-points according to the Monkhorst–Pack scheme and the electronic and atomic relaxations are carried out using either a conjugate gradients or BFGS algorithm. Two computer programs are used which implement this methodology: CASTEP [12] and DACAPO [13]. The grain boundaries are constructed within supercells which are oriented appropriately so as to contain one repeat unit of the structure and this is determined by the coincidence site lattice (CSL) [14]. Two different boundary geometries are considered: the $\Sigma = 13$ ($\theta = 32.2°$) [0001] tilt boundary and the $\Sigma = 7$ ($\theta = 21.8°$) [0001] twist boundary. The $\Sigma$ parameter defines the periodicity of the boundary which for the tilt geometry is $a_0\sqrt{13}$ and for the twist geometry is $a_0\sqrt{7}$ where $a_0$ is the ZnO lattice constant equal to 3.23 Å. However, because of the different boundary orientations, the interfacial areas per unit CSL cell are about the same: 60.33 Å$^2$ for the tilt boundary and 63.25 Å$^2$ for the twist boundary. Supercells are used to perform the calculations and thus each system contains two symmetry-equivalent grain boundaries. The model sizes used are 104 and 112 atoms for the tilt and twist boundaries respectively.

The simulation of Bi segregation to each boundary is accomplished by substitutional replacement of Zn atoms in the core of each structure. By varying the number of substitutions that are made, the local Bi concentration is determined. For the tilt boundary, which contains 16 Zn atoms in its core, 1–6 different Zn sites are replaced with Bi atoms resulting in a maximum local Bi concentration of 37.5% (or 18.75 at.%). For the twist boundary, which contains 14 Zn atoms in its core, 1–5 different Zn sites are replaced with Bi atoms resulting in a maximum local Bi concentration of 35.7% (or 17.85 at.%). Depending on how the Bi atoms are distributed in the boundaries, these maximum concentrations can correspond to approximately one monolayer of segregated impurity. The results are analysed by examining the effects of

Bi segregation on the boundary structures, the densities of states, the Mulliken charges, the effective potential barriers and the segregation energies. Both total densities of states and atom-resolved partial densities of states are obtained. The Mulliken charges are determined from a population analysis based on projecting the Kohn–Sham eigenstates onto atomic orbital basis sets [15]. Information about the potential barriers is obtained by mapping the effective one-electron potential across the supercell normal to each boundary. The segregation energies are determined by computing the Bi substitution energies in the grain boundary and the bulk and subtracting them [16]. The bulk substitution is considered in the dilute, non-interacting limit.

## 3. Results

The atomic and electronic structures of the *undoped* $\Sigma = 13$ and 7 grain boundaries have been determined by us in previous studies [17, 18]. In both cases, two distinct equilibrium structures similar in energy were discovered. For the $\Sigma = 13$ tilt boundary, one of these structures was found to be consistent with high-resolution electron microscope observations [19] and this is the structure considered here. This structure is characterized by a zigzag chain of ten-atom rings with each ring containing two dangling bonds, i.e. two three-coordinated sites. These dangling bonds create electron states just on the top valence band maximum for the oxygen atoms, but since they are occupied they cannot act as acceptor states. For the $\Sigma = 7$ twist boundary, one of the low-energy structures results from a rotation in which the boundary plane cuts through polar Zn–O bonds and this is the structure considered here. It is characterized as well coordinated with no dangling bonds despite the twist misorientation. The average bond length across the boundary increases by a small amount (5.7%), which has the main effect of broadening the valence and conduction bands slightly. Like in the case of the $\Sigma = 13$ tilt boundary, no deep acceptor states appear in the band gap and this is consistent with $I$–$V$ measurements for undoped [0001] twist boundaries in ZnO [20]. Starting with the undoped structures for the $\Sigma = 13$ and 7 grain boundaries, Zn atoms in the boundary cores are replaced with increasing numbers of Bi atoms up to the maximum concentrations specified above. The following is a summary of the results for each boundary.

### *3.1. Bi decoration of the* $\Sigma = 13$ *tilt boundary*

The boundary was decorated with up to six Bi atoms distributed among three different core sites which are labelled A, B and C in figure 1. A is one of the three-coordinated sites at the neck of a ten-atom ring and B and C are two different four-coordinated sites. Substitution of a single Bi atom, which corresponds to a local concentration of 6.25%, showed that the A site is the most energetically preferred. The A site allows greater freedom for relaxation of the larger Bi atom which moves slightly into the ten-atom ring. The segregation energy is $-1.22$ eV and indicates a significant driving force for segregation. The propensity for segregation continues as further sites are populated with Bi. Figure 2 shows the variation of segregation energy for various distributions of Bi in the boundary up to the maximum local concentration of 37.5%. Only those configurations giving the largest segregation energy at a particular concentration are plotted. The figure shows that the strongest segregation occurs for two or three Bi atoms in A sites and that beyond five Bi substitutions (AAAAB, corresponding to 31.25%) the segregation energy goes positive and the process becomes unfavourable. The upturn in segregation energy after three Bi atoms have segregated is caused by the repulsive Bi–Bi interaction which gets stronger as the Bi concentration increases. To diminish this interaction a Bi–Bi bond forms across the ring structure when two Bi atoms occupy adjacent three-coordinated sites. This leads to charge accumulation in the doped tilt boundary.

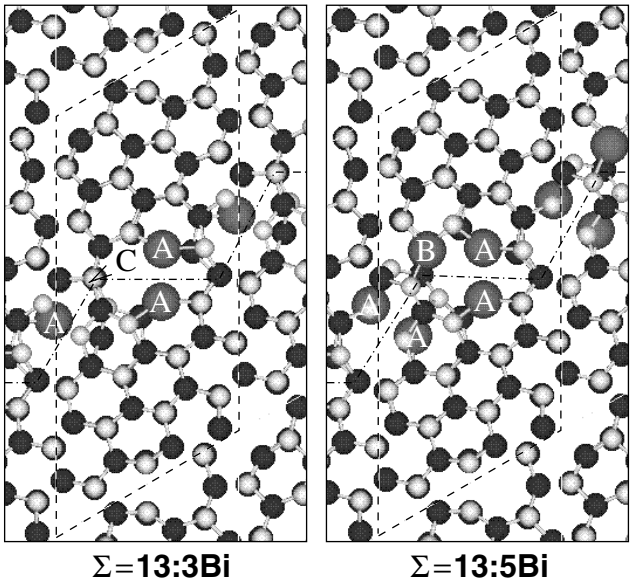


**Figure 1.** The relaxed structures of a $\Sigma = 13$ tilt boundary in ZnO containing three and five Bi atoms. The segregation sites are labelled A and B. Site C is another site also considered for substitution. The structures are viewed down the [0001] tilt axis with Zn atoms drawn black and O atoms drawn white. The dash–dot line indicates the position of the boundary and the dashed line outlines the limits of the supercell.

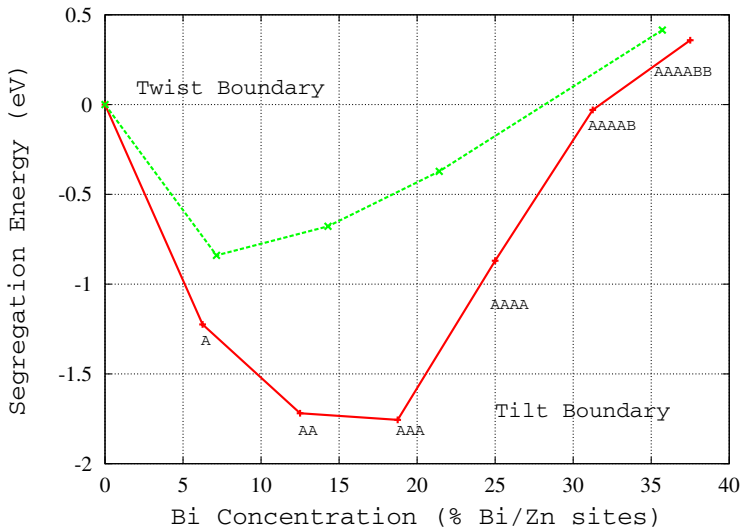


**Figure 2.** The Bi segregation energies as a function of Bi concentration for the $\Sigma = 13$ tilt boundary (full curve) and the $\Sigma = 7$ twist boundary (dashed line). The letters on the full curve refer to the substitution sites in the tilt boundary shown in figure 1.

The effects of Bi decoration on the electronic structure of the boundary were studied by analysing the partial density of states (PDOS), the electron density distributions and the effective one-electron potential across the supercell. When a single Bi atom segregates to the

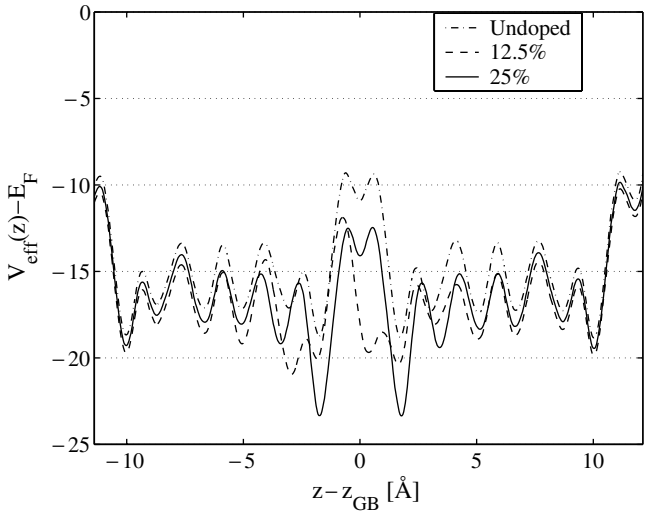


**Figure 3.** The effective one-electron potential normal to the $\Sigma = 13$ tilt boundary for Bi doping concentrations of 0, 12.5 and 25%. The boundary is located in the centre of the diagram with periodic images at the ends. Doping the boundary increases the local potential which becomes more negative in planes adjacent the boundary core.

boundary it donates a fraction of its p electrons to the conduction band. The band gap does not contain any states and the Fermi level is located in the conduction band, resulting in a metallic system with the metallicity probably localized in the grain boundary plane. When the Bi concentration is increased, Bi–Bi interactions pull the p states closer to the Fermi level. This indicates that the Bi atoms are retaining more charge and it is more favourable for them to form a Bi–Bi bond. The charge density distribution between neighbouring Bi atoms in the boundary shows bond formation and the PDOS indicates that these bonds have $\sigma$-character and reside deep in the band gap. Thus the formation of Bi–Bi bonds at high Bi concentrations leads to electron localization in the grain boundary. It is interesting that the donor behaviour observed at low Bi concentrations disappears as more Bi segregates to the boundary due to the formation of impurity–impurity bonds. The accumulation of electrons at the boundary will result in a potential barrier. Although the actual potential barrier cannot be calculated using the present methodology, it can be represented by the effective one-electron potential in the supercell mapped normal to the boundary. This is shown in figure 3 for the undoped boundary and for the boundary containing 12.5 and 25% Bi. It is seen that both the undoped and doped boundaries increase the local potential, i.e. it becomes more negative. For the boundary with 25% Bi, the disturbance in the potential seems to be greatest in planes adjacent to the boundary.

### *3.2. Bi decoration of the $\Sigma = 7$ twist boundary*

The boundary was decorated with up to five Bi atoms distributed within the two (0001) Zn planes adjacent to the twist boundary. A plan view of the boundary along [0001] is shown in figure 4 which illustrates two examples in which (a) three Bi atoms and (b) five Bi atoms are incorporated into the same (0001) plane. These substitutions correspond to local concentrations of 21.4 and 35.7% respectively. A population of seven atoms all situated in one (0001) plane would correspond to a complete monolayer of Bi. The number of ways of populating the boundary with Bi is very large and it has not been possible to study them all. In the present study the following substitutions have been investigated: a single Bi atom; two Bi atoms either

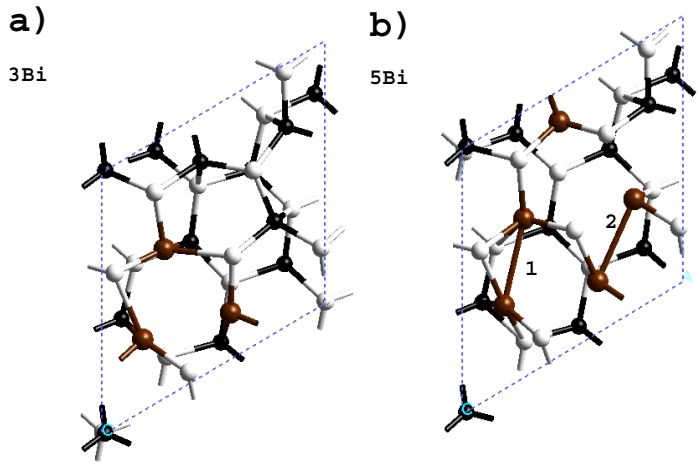


**Figure 4.** The relaxed structures of a $\Sigma = 7$ twist boundary in ZnO containing (a) three Bi and (b) five Bi atoms. The structures are viewed down the [0001] twist axis showing two planes above and two planes below the boundary. Zn, O and Bi atoms are drawn black, white and grey respectively. The dotted line indicates the limits of the supercell. Two new Bi–Bi bonds labelled 1 and 2 are illustrated.

in the same plane or in adjacent planes; three Bi atoms either in the same plane or two in the same plane and one in an adjacent plane; five Bi atoms all in the same plane. Only non-CSL sites were considered for substitution. Unlike the tilt boundary, all sites in the twist boundary are four-coordinated. Substitution of a single Bi atom resulted in a segregation energy of $-0.84$ eV indicating a driving force for segregation which is somewhat lower than in the tilt boundary. Substitution of two or three Bi atoms (all in the same plane) also resulted in negative segregation energies as shown in figure 2. Once again only those configurations giving the largest segregation energy at a particular concentration are plotted. However, when five Bi atoms are introduced into the boundary (all in the same plane) it is found that the segregation energy becomes positive, indicating that this distribution and concentration is unfavourable. Figure 2 shows that the strongest segregation occurs for one or two Bi atoms and that beyond three Bi substitutions (corresponding to 21.4%) decoration will not continue. However, it is emphasized that not all possible Bi distributions have been studied. As for the tilt boundary, the upturn in segregation energy is caused by a repulsive Bi–Bi interaction which increases as the Bi concentration increases. This interaction is diminished somewhat in cases where Bi–Bi bonds form. For example, when two Bi atoms are substituted in adjacent planes across the boundary, a strong bond forms which reduces the segregation energy to $-0.15$ eV (not shown in figure 2).

The effects of Bi decoration on the electronic structure of the boundary were studied by analysing the Mulliken charges and populations and by calculating the effective one-electron potential across the supercell. The Mulliken charges on all atoms in planes adjacent to the boundary were determined. It was found that the incorporation of Bi atoms decreased the average Mulliken charge in the planes near the substitution indicating a local accumulation of charge. The bond populations were also calculated and it was found that when Bi–Bi bonds formed within the boundary core their overlap populations were significantly larger than those of the Zn–O bond in the bulk (=0.33e). For example, the bond referred to above for two Bi atoms across the boundary has a population of 0.74e. Also when five Bi atoms are substituted in the same plane, two new bonds form with populations of 0.88e and 0.36e as illustrated in

figure 4. Bonds between Bi atoms and Zn atoms are also observed. As in the tilt boundary, the accumulation of electrons in the twist boundary should result in a potential barrier. The effective one-electron potential has been determined and is found to have features qualitatively similar to that shown in figure 3.

## 4. Discussion and conclusions

The calculations clearly show a strong driving force for the segregation of Bi atoms to both types of grain boundary. For the $\Sigma = 13$ tilt boundary, a maximum local Bi concentration of about 32% can be achieved before further segregation becomes unfavourable. For the $\Sigma = 7$ twist boundary, a maximum local Bi concentration of about 28% can be achieved. Interestingly, the maximum concentrations are about the same and this is perhaps related to the fact that the densities of Zn atoms in the boundary cores are also about the same, as are the unit areas. In both cases, the boundaries can become decorated with only a fraction of a monolayer of Bi and this is consistent with experimental observations which suggest that on average 0.5 monolayers cover general boundaries in Bi-doped ZnO, at least in samples equilibrated at 725 °C [21]. Accompanying Bi decoration is charge accumulation. This is evident in the PDOS analysis of the tilt boundary and the Mulliken population analysis of the twist boundary. The PDOS analysis shows that the Bi atoms retain more charge in the boundary and tend to form Bi–Bi bonds if the local concentration is high enough. The population analysis shows that the average Mulliken charges on planes adjacent to those containing Bi atoms reduce in magnitude, implying that they have also retained more charge. Associated with charge accumulation at the boundaries should be potential barriers. The present methodology cannot be used to determine the true height or shape of these barriers, but as an approximate guide the one-electron potentials across the supercell normal to the boundaries have been extracted from the calculations and these show significant disturbances at the interface. For both boundaries the potential variation increases locally and extends to at least one plane on either side of the interface.

Although the present study has demonstrated the existence of potential fluctuations and charge accumulation at grain boundaries doped with Bi, no evidence has been found for deep defect levels of acceptor type that are associated with the Schottky barrier model. In this model, acceptor levels are needed to trap electrons and then release them when a critical breakdown field is applied. The present results suggest an alternative model in which electrons are trapped in Bi–Bi bonds and it is these bond populations that are depleted in an external field. However, it may be that depletion of acceptor levels is energetically easier than depletion of metal bonds, and therefore further calculations are necessary to determine whether more complex defect configurations generate the required levels. In particular, it is known that oxidation of doped grain boundaries increases the non-linear effect in ZnO and that this can be reversed on reduction [5]. Up to a monolayer of oxygen can adsorb onto the doped grain boundaries, creating an oxygen-rich environment in which Zn vacancy formation may be preferred. It is therefore possible that the chemical origin of the acceptor state in the Schottky barrier model is a complex of Zn vacancies, O interstitials and Bi substitutionals all segregated at grain boundaries. Further calculations are in progress to examine this possibility.

## Acknowledgments

JC was supported by the Swedish Natural Science Research Council and HSD acknowledges grant PRAXIS XXI/BD/13944/97. The calculations were performed using the CSAR (Manchester) and UNICC (Gothenburg) computing facilities.

## References


[1] Look D C 2001 *Mater. Sci. Eng.* B **80** 383
[2] Levinson L M and Philipp H R 1991 *Ceramic Materials for Electronics* ed R C Buchanan (New York: Dekker) p 349
[3] Clarke D R 1999 *J. Am. Ceram. Soc.* **82** 485
[4] Chiang Y-M, Wang H and Lee J-R 1998 *J. Microsc.* **191** 275
[5] Greuter F, Blatter G, Rossinelli M and Stucki F 1989 *Ceram. Trans.* **3** 31
[6] Hozer L 1994 *Semiconductor Ceramics—Grain Boundary Effects* (New York: Ellis Horwood)
[7] Oba F, Tanaka I, Nishitana S R, Adachi H, Slater B and Gay D H 2000 *Phil. Mag.* A **80** 1567
[8] Oba F and Adachi H 2000 *J. Mater. Res.* **15** 2167
[9] Payne M C, Teter M P, Allan D C, Arias T A and Joannopoulos J D 1992 *Rev. Mod. Phys.* **64** 1045
[10] Perdew J, Chevary J, Vosko S, Jackson K, Pederson M, Singh D and Fiolhais C 1992 *Phys. Rev.* B **46** A6671
[11] Vanderbilt D 1990 *Phys. Rev.* B **41** 7892
[12] *Cerius*$^2$ *User Guide* 1999 MSI/Accelrys
[13] Hammer B *et al* 1998 *DACAPO-1.30* Centre for Atomic Scale and Materials Physics, Danmarks Tekniske Universitet, Lyngby, Denmark
[14] Bollmann W 1970 *Crystal Defects and Crystalline Interfaces* (Berlin: Springer)
[15] Segall M D, Pickard C J, Shah R and Payne M C 1996 *Mol. Phys.* **89** 571
[16] Carlsson J M, Hellsing B, Domingos H S and Bristowe P D 2002 *Surf. Sci.* at press
[17] Carlsson J M, Hellsing B, Domingos H S and Bristowe P D 2001 *J. Phys.: Condens. Matter* **13** 9937
[18] Domingos H S and Bristowe P D 2001 *Comput. Mater. Sci.* **22** 38
[19] Kiselev A, Sarrazit F, Stepantsov E, Olsson E, Claeson T, Bondarenko V, Pond R and Kiselev N 1997 *Phil. Mag.* A **76** 633
[20] Sato Y, Oba F, Yamamoto T, Ikuhara Y and Sakuma T 2002 *J. Am. Ceram. Soc.* **85** 2142
[21] Lee J-R, Chiang Y-M and Ceder G 1997 *Acta Mater.* **45** 1247